IET Optoelectronics

Research Article

IET Journals
The Institution of Engineering and Technology

Modelling and simulation of novel liquid-infiltrated PCF biosensor in Terahertz frequencies

ISSN 1751-8768
Received on 19th April 2020
Revised 7th July 2020
Accepted on 23rd July 2020
E-First on 4th September 2020
doi: 10.1049/iet-opt.2020.0069
www.ietdl.org

Nurul Awadah Nadiah Binti Suhaimi[1], *Izaddeen Kabir Yakasai*[1] ✉, *Emeroylariffion Abas*[1], *Shubi Kaijage*[2], *Feroza Begum*[1]

[1]*Faculty of Integrated Technologies, Universiti Brunei Darussalam, Jalan Tungku Link BE1410, Bandar Seri Begawan, Brunei*
[2]*School of Computational and Communications Science and Engineering (CoCSE), the Nelson Mandela African Institution of Science and Technology (NM-AIST), Arusha, United Republic of Tanzania*
✉ *E-mail: 17h0892@ubd.edu.bn*

Abstract: The liquid-infiltrated photonic crystal fibre (LI-PCF) is proposed for guiding terahertz radiation. Geometrical asymmetry is achieved by introducing a large ellipse in the core. By filling the ellipse with liquid cocaine, the optical properties of the photonic crystal fibre (PCF) are theoretically examined using finite element method-based COMSOL multiphysics software. At an operating frequency of 1 THz, the proposed LI-PCF demonstrates a sensitivity of 87.02% and confinement loss in the order of 10^{-4} cm^{-1}. The PCF also demonstrates extremely low effective material loss <0.01 cm^{-1}, a birefringence of 0.018, large effective mode area of 1.11×10^5 μm^2, a high numerical aperture of 0.45 and near-zero ultra-flattened chromatic dispersion of 1.4351 ± 0.5883 ps/THz/cm. The design simplicity and high sensitivity, strong confinement factor, low material losses and high birefringence of the fibre suggest that the proposed fibre may be convenient for PCF-based cocaine sensing, for application in the security and defence industries.

1 Introduction

Cocaine, in the form of powder or liquid, has stimulant and euphoric properties that induces a high level of euphoric dependence on its user and subsequently, illicit use. Difficulties associated with the detection and identification of liquid cocaine have motivated the development of several optical techniques. Some of these techniques include the use of fibre-optic biosensors for sensing cocaine leaf extracts [1], the use of infrared spectroscopy for identification of the absorption spectra of cocaine [2] and the use of quantum cascade laser (QCL) and fibered absorption cell for sensing traces of cocaine and its concentration [3]. Another possible optical method that has been developed for detection involves the use of photonic crystal fibres (PCFs).

PCFs are special optical fibres that consist of neatly arranged micrometre-scaled air hole discontinuities stretching across the entire fibre length [4]. Light guidance in PCFs is achieved by either photonic bandgap effect or total internal reflection mechanisms. PCFs are capable of offering excellent light guidance properties such as extremely low confinement loss [5], near-zero ultra-flattened chromatic dispersion [6], high sensitivity [7], large non-linearity [8] and effective mode area [9]. Furthermore, optical properties of PCFs can be adapted to various applications by fine-tuning the shape, size and position of the air hole discontinuities. Thus, PCFs have found applications in many areas, including biomedicine [10], spectroscopy [11], security [12], telecommunication [13] etc.

In the last decade, several liquid sensors based on various PCF geometries for operation in the optical regime, have been proposed. Wu *et al.* [14] proposed a microfluidic refractive index sensor based on fluidic infiltration into a single air hole. At the same time, Park *et al.* [15] investigated the optical properties of a chemical sensor with a relative sensitivity of 5.09%. An octagonal lattice PCF sensor for operation in the optical region was proposed by Ahmed *et al.* [16] and its propagation characteristics analysed; showing relative sensitivity <50% within the 0.5–2 μm wavelength band. Subsequently, a slight improvement in relative sensitivity has been achieved by Islam *et al.* [17]. The sensor based on a hexagonal cladding lattice and circular core lattice has shown relative sensitivity of 53.22% within 1.0–1.7 μm wavelength region. Consequently, Islam *et al.* [18] reported a hexagonal-shaped PCF sensor for plasma sensing applications. The sensor showed a relative sensitivity of 77.84% at 1.3 μm operating wavelength.

Recently, various researchers have proposed PCF-based sensors for operation in the terahertz regions; with improved losses and sensitivity profiles. Various research groups have proposed PCF-based sensors for THz sensing applications [12, 19–21]. Islam *et al.* [19] proposed an ethanol sensor consisting of kagome-cladding lattice and a rectangular slotted core, and have shown birefringence of 5×10^{-3}, the high relative sensitivity of 85.7% and confinement loss of 1.7×10^{-9} cm^{-1}. However, effective material loss (EML) – a measure of the amount of light absorbed by the background material per unit length, of the fibre has not been assessed.

The same group of researchers [20] also proposed a terahertz PCF sensor for alcohol detection with birefringence of 1.65×10^{-2}, the relative sensitivity of 68.87%, confinement loss 6.12×10^{-12} cm^{-1} and EML of 0.055 cm^{-1}. However, the fibre consists of 88 cladding air holes and nine microstructure-scaled ellipses in the core; adding to the fabrication complexity due to a large number of air holes. A PCF with elliptical core air holes and suspended cladding has been proposed for detecting cyanide in terahertz frequencies [21]. The birefringence of the reported fibre is 4.9×10^{-2}, with relative sensitivity, confinement loss and EML of 77.5%, 5.15×10^{-8} and 0.031 cm^{-1}, respectively. Nevertheless, the authors have not thoroughly considered the impact of air holes size and position on the obtained transmission and sensitivity profiles during parameter optimisation. An elliptical core PCF was proposed for sensing liquid warfare agents [12]. The sensor showed with relative sensitivity, confinement loss and EML of 64%, 10^{-12} and 0.028 cm^{-1}, respectively. The number of elliptical air holes in the core and circular cladding air holes was reduced to ease the fabrication complexity,

With an increased need for reduced PCF fabrication complexity, herein, a novel PCF with two cladding rings and a single elliptical liquid channel is presented for sensing liquid cocaine in terahertz frequencies. The single elliptical liquid channel offers improved

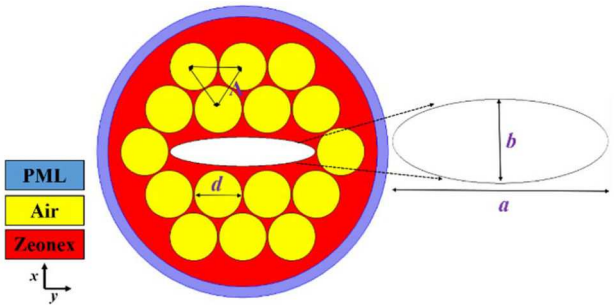

Fig. 1 *Geometrical spatial extent of the proposed sensor with an enlarged view of the elliptical core indicating the major axis a and minor axis b*

sensitivity and confinement factor due to enhanced light-matter interaction. Moreover, the ellipse introduces the birefringence effect and reduces the loss of light to material absorption.

2 Geometrical architecture of the proposed sensor

The cross-sectional geometry of the proposed sensor is presented in Fig. 1, with an enlarged view of the hollow elliptical core. Birefringence is essential for sensing, and it is achieved by artificially destroying geometrical symmetry of the PCF. As such, a large ellipse is introduced in the core, with parameters a and b representing major and minor axes of the ellipse, respectively. The major axis, a, is kept fixed at 370 µm. In contrast, the minor axis, b, is varied throughout the iterative simulation process to observe its impact on the optical properties of the PCF. The cladding design follows a hexagonal lattice consisting of 4 and 12 equally sized circular air holes in the first and second rings, respectively. The diameter of each cladding air hole is denoted by d, and the distance between centres of adjacent air holes or its pitch is denoted by Λ. Air filling fraction, which is the ratio of air hole diameter to pitch, is set to 0.97, i.e. $\Lambda = d/0.97$.

In the past, photonics engineers have used various dielectric materials as the substrate for designing THz PCF sensors. Some of these substrate materials include Polymethyl-methacrylate, Tetrafluoroethylene and cyclic olefins (Topas and Zeonex) [6, 12]. Cyclic olefins have flat refractive index profile ($n \simeq 1.53$) within a wide terahertz frequency range, resulting in negligible material dispersion. They also have a low bulk absorption coefficient of 0.2 cm^{-1} at 1 THz. Among cyclic olefins, Zeonex has better biocompatibility and chemical resistance at higher temperatures, high glass transition temperature and negligible moisture absorption. Therefore, Zeonex has been selected as the substrate material of the proposed PCF.

Perfectly matched layer (PML) has been imposed outside the cladding region, which acts as an anti-reflective layer that absorbs outgoing waves; preventing light from reflecting onto the fibre. PML thickness is optimised at 8% of the cladding diameter, after careful trial and error iterations it showed a negligible effect of PML thickness on the confinement loss.

3 Simulation method and numerical synopsis

The full vector finite element method (FEM)-based COMSOL multiphysics software is used for numerical analysis of the proposed PCF. FEM utilises meshing technique to divide the PCF's geometry into 7724 smaller triangles called elements. It then combines Maxwell wave equations and PML absorbance boundary condition to solve the formulated elements individually. The elliptical core is filled with liquid cocaine having a relatively flattened refractive index of $n_r \simeq 1.5022$ [22] and negligible absorption coefficient within 0.4–1.6 THz [23]. Then, confinement loss, power fraction and relative sensitivity are examined within the 0.4–1.6 THz frequency range and ellipse minor axis lengths b of 55, 75 and 95 µm.

The PCF needs to be able to confine as much light as possible in its core. Mode field or light confinement is measured by the confinement loss property, which is dependent on the imaginary part of the complex effective refractive index. Confinement loss is expressed as [6]:

$$L_c(\mathrm{cm}^{-1}) = 8.686\left(\frac{2\pi f}{c}\right)\mathrm{Im}[n_{\mathrm{eff}}] \times 10^{-2}\,\mathrm{cm}^{-1} \tag{1}$$

where f is the operating frequency, $\mathrm{Im}[n_{\mathrm{eff}}]$ is the imaginary part of the complex effective refractive index and $c = 3 \times 10^8$ m/s is the speed of light in vacuum.

The amount of power propagating through the infiltrated cocaine sample is quantified by the power fraction parameter K and it is expressed as [12]

$$K = \frac{\int_x S_z \mathrm{d}A}{\int_{\mathrm{all}} S_z \mathrm{d}A} \times 100\% \tag{2}$$

where S_z is the z-component of the Poynting vector projecting in the propagation direction, the integral in the numerator is computed over the region filled with the liquid cocaine. In contrast, the denominator integral is computed over all-fibre regions.

Relative sensitivity is obtained by applying modified Beer–Lambert law to determine the degree of interaction between excited terahertz pulses and the infiltrated liquid cocaine sample. Relative sensitivity determines how sensitive the proposed PCF is, and it is expressed as [24]

$$r = \frac{n_r}{\mathrm{Re}[n_{\mathrm{eff}}]} \times K \tag{3}$$

where $n_r = 1.5022$ is the refractive index of cocaine and $\mathrm{Re}[n_{\mathrm{eff}}]$ denotes the real part of the effective refractive index.

The amount of terahertz light absorbed by the background Zeonex per unit length is known as EML, and it may arise due to loss of material molecules resulting from heat generated from increased light-matter interaction. EML is expressed as [6, 25]

$$\alpha_{\mathrm{eff}} = \sqrt{\frac{\varepsilon_0}{\mu_0}}\left(\frac{\int_{\mathrm{mat}} n_{\mathrm{mat}} |\boldsymbol{E}|^2 \alpha_{\mathrm{mat}} \mathrm{d}A}{2\int_{\mathrm{All}} S_z \mathrm{d}A}\right) \tag{4}$$

where ε_0 and μ_0 represent the permittivity and permeability of free space, respectively. $n_{\mathrm{mat}} = 1.53$ is the Zeonex's refractive index, $\boldsymbol{E}$ denotes the electric field of the fundamental mode and $\alpha_{\mathrm{mat}} = 0.2$ cm^{-1} is the bulk material absorption loss. Since most of the core is occupied by liquid cocaine analyte, it is expected that the EML will be low. Furthermore, the absorption coefficient of liquid cocaine sample within the examined frequency range, i.e. 0.4–1.6 THz, is negligible. Polarisation preservation is essential for PCF-based sensors, requiring high birefringence [38]. High birefringence may be achieved by disrupting geometrical symmetry of the PCF, in this case, by introducing a large ellipse in the core region. Birefringence property is calculated using the following expression [25]

$$B = \left|n_{\mathrm{eff}}^x - n_{\mathrm{eff}}^y\right| \tag{5}$$

where n_{eff}^x and n_{eff}^y denote the real components of the effective refractive index of x and y fundamental modes.

The total area covered by the hat-like Gaussian beam is called the effective area, and it is measured using the following expression [6]:

$$A_{\mathrm{eff}} = \frac{\left[\int I(r) r \mathrm{d}r\right]^2}{\int I^2(r) r \mathrm{d}r} \tag{6}$$

where $I(r)$ denotes the distribution of electric field intensity in the transverse direction.

Numerical aperture is an important dimensionless PCF parameter that depends on the core-cladding refractive index

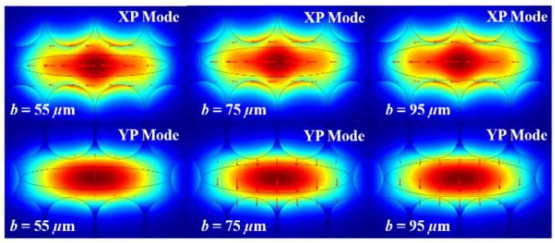

Fig. 2 *Electric field distribution of the proposed PCF at different minor axis lengths, with the direction of mode field propagation in the x and y polarisation modes indicated by the horizontal and vertical red arrows, respectively*

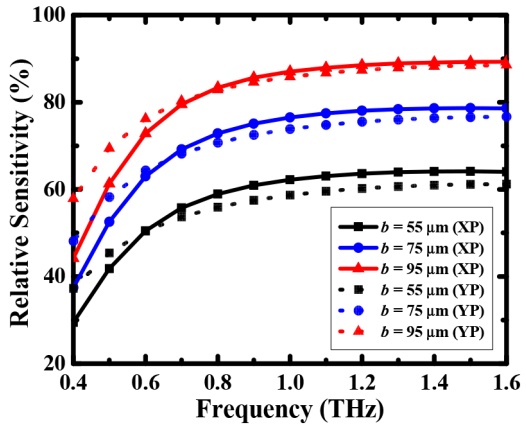

Fig. 3 *Relative sensitivity with respect to frequency for x and y polarisation modes at different minor axis length values*

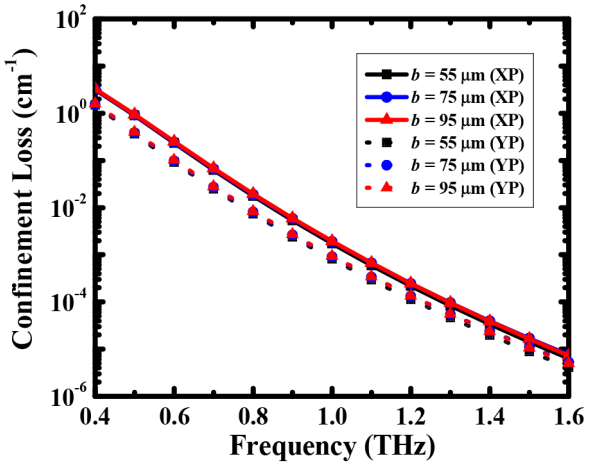

Fig. 4 *Confinement loss with respect to frequency for x and y polarisation modes at different minor axis length values*

contrast, with PCF sensing application requiring a large numerical aperture. It is defined using the following expression [26]:

$$\mathrm{NA} \simeq \frac{1}{\sqrt{1+((\pi A_{\mathrm{eff}} f^2)/c^2)}} \tag{7}$$

where A_{eff}, f and c denote effective area, operating frequency and speed of light in vacuum, respectively.

Group velocity dispersion (GVD) is a parameter that helps define the PCF's information-carrying capacity, and it is a summation of the background material and waveguide dispersion. However, since Zeonex has intrinsically negligible dispersion due to stable refractive index in terahertz frequencies, only waveguide dispersion is considered for the proposed PCF. Waveguide dispersion can be calculated using the following expression [6, 12]:

$$\beta_2 = \frac{2}{c}\frac{\mathrm{d}n_{\mathrm{eff}}}{\mathrm{d}\omega} + \frac{\omega}{c}\frac{\mathrm{d}^2 n_{\mathrm{eff}}}{\mathrm{d}\omega^2} \tag{8}$$

where c denotes the speed of light in vacuum, n_{eff} and ω denote the effective refractive index of the fundamental mode and angular frequency, respectively.

4 Results and discussion

Electric field distributions for different minor axis at 1 THz operating frequency for x and y polarisation modes are presented in Fig. 2. The figure illustrates a strong mode field confinement at the core – inside the cocaine sample. This interaction results in high sensitivity, with low confinement and EMLs. It can also be seen from the figure that stronger mode field confinement is obtained as minor axis length is increased, especially in the y polarisation mode.

Fig. 3 shows the relative sensitivity of the proposed PCF at different minor axis lengths with respect to frequency. It can be observed that relative sensitivity rapidly increases with increasing frequency at lower frequency region (0.4–0.8 THz) but subsequently flattens towards the upper region (0.8–1.6 THz) of the examined frequency spectrum. This phenomenon is partly due to the incremental rate of the effective refractive index as the frequency increases. Based on (3), the relative sensitivity is dependent on the refractive index of cocaine and power fraction.

An increase in the frequency leads to an increase in the refractive index and power fraction. Thus, the relative sensitivity increases. Also, since the relative sensitivity is dependent on the incremental rate of the effective refractive index, then an increase in the effective refractive index will lead to a decline in the relative sensitivity. Therefore, when the relative sensitivity increases, power fraction must increase at a faster pace than the effective refractive index.

Also, higher relative sensitivity is observed with more considerable minor axis length due to increased power fraction resulting from the stronger terahertz light interaction with cocaine. It is noticeable that while the x polarisation mode's relative sensitivity is higher for most of the examined frequency spectrum, the y polarisation mode exhibits higher relative sensitivity at lower frequencies, specifically within 0.4–0.6 THz at $b = 75$ μm and within 0.4–0.7 THz at $b = 55$ μm and $b = 95$ μm. These variations occur due to the higher power fractions in the y polarisation mode at these minor axis lengths and frequencies. Relative sensitivities of 87.02 and 85.82% are obtained with $b = 95$ μm at 1 THz operating frequency for x and y polarisation modes, respectively.

The confinement loss profile with respect to the frequency at different values of b, for x and y polarisation modes, is presented in Fig. 4. Logarithmic reduction in confinement loss is observed as frequency increases, due to stronger terahertz light interaction with cocaine. Furthermore, both polarisation modes demonstrate negligible confinement losses at higher frequencies. With $b = 95$ μm and 1 THz operating frequency, confinement losses of the proposed sensor are 1.95×10^{-3} and 9.42×10^{-4} cm^{-1} for the x and y polarisation modes, respectively.

EML is examined for the orthogonal modes in Fig. 5 for different values of b. The figure shows EML reducing with an increase in the minor axis length. Increasing the minor axis length value replaces the Zeonex present in the core region with cocaine, thus ensuring more interaction between sample cocaine and terahertz light. A flattened EML profile for all minor axis length is also observed, thus further proving the potential of the proposed fibre as a low loss terahertz waveguide and cocaine sensor. With $b = 95$ μm and 1 THz frequency, the proposed fibre shows extremely low EMLs of 0.009 and 0.012 cm^{-1} for x and y polarisation modes, respectively.

High birefringence helps in ensuring smooth waveguiding and sensing operation by removing polarisation mode dispersion effects, and it may be done by breaking structural symmetry of the fibre. In the proposed sensor, birefringence is induced via the introduction of the ellipse in the core. Birefringence of the proposed fibre between 0.4 and 1.6 THz frequency range is presented in Fig. 6, with birefringence from 0.9 to 1.1 THz given in

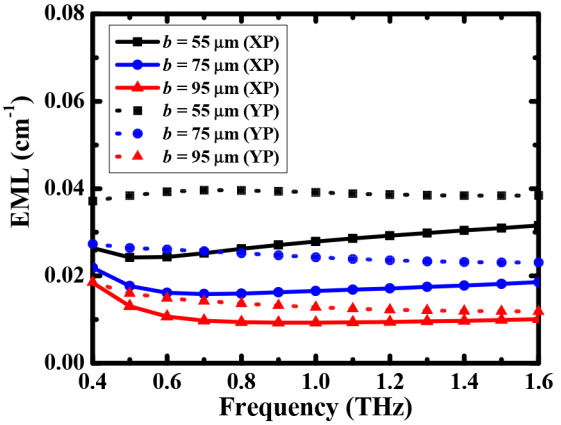

Fig. 5 *EML with respect to frequency for x and y polarisation modes at different minor axis length values*

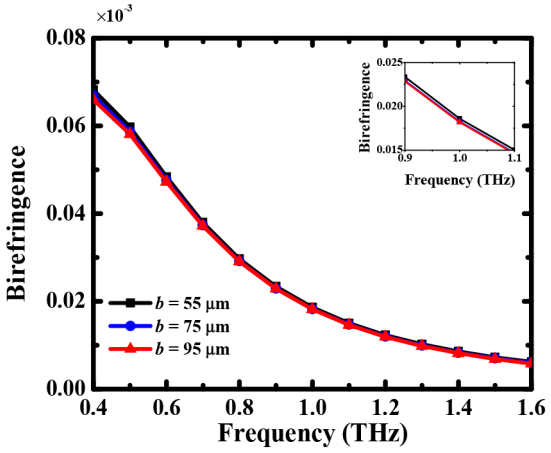

Fig. 6 *Birefringence of proposed PCF at different minor axis length*

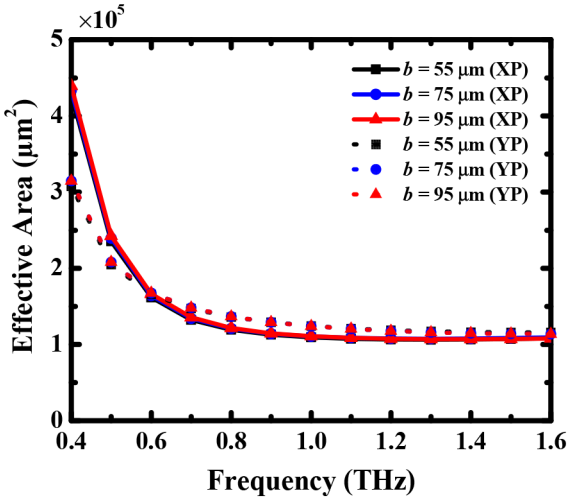

Fig. 7 *Effective area with respect to frequency, for x and y polarisation modes at different minor axis length values*

the inset. At minor axis length $b = 95$ μm and 1 THz operating frequency, birefringence is 1.8×10^{-2}; a tiny reduction from the maximum birefringence with $b = 55$ μm and considerably high compared to previously proposed PCF-based THz sensors [14–17]. Furthermore, relative sensitivity is highest at $b = 95$ μm for 1 THz operating frequency. Thus, $b = 95$ μm is selected as the preferred minor axis length for the proposed sensor.

Effective area and numerical aperture of the proposed fibre with respect to the frequency at different minor axis length, for x and y polarisation modes, is shown in Figs. 7 and 8. Generally, both effective area and numerical aperture reduce with increase in frequency. As the frequency is increased, guided terahertz light confines more tightly in the cocaine-filled core thus, reducing the effective area covered by the fundamental mode. Similar trends are observed for numerical aperture since the numerical aperture is dependent on the effective area, as shown in (6). The x-polarisation mode is observed to have a higher effective area at lower operating frequencies, however, is later surpassed by the y polarisation mode at a higher frequency. At 1 THz operating frequency and $b = 95$ μm, effective areas for the x and y polarisation modes are 1.11×10^5 and 1.24×10^5 μm^2, respectively, while numerical apertures are 0.45 and 0.43 for x and y polarisation modes, respectively.

Dispersion profile of the proposed PCF for x and y polarisation modes at various minor axis length is presented in Fig. 9. As has been previously discussed, dispersion is mainly determined by the waveguide dispersion. It can be seen that the proposed PCF gives higher dispersion at a lower frequency, with dispersion approaching zero as the frequency is increased. Also, the y polarisation mode gives lower dispersion throughout the examined frequency spectrum. The waveguide's x-polarisation dispersion magnitude at 1 THz and $b = 95$ μm is 1.6456 ps/THz/cm while for the y polarisation mode, it is 1.2689 ps/THz/cm. Moreover, the obtained dispersion profiles across the examined frequency spectrum for the x and y polarisation modes are 1.8760 ± 0.8067 and 1.4351 ± 0.5883 ps/THz/cm, respectively.

Finally, the properties of the proposed PCF sensor are tabulated in Table 1 and compared with previously proposed sensors in the literature. From the table, the proposed PCF shows the highest relative sensitivity and birefringence. Comparison with other sensors which optimised at the same 1 THz operating frequency, shows that the proposed PCF sensor gives better guidance properties, in terms of relative sensitivity, birefringence and EML. No comparison with other liquid cocaine PCF sensor is possible, due to the non-existence of this kind of sensor in the literature.

5 Fabrication and sensing mechanism

The advantage of the proposed biosensor in comparison to existing THz biosensors [27] in the literature lies in its design simplicity. Some existing biosensors rely on the phenomenon of surface plasmon resonance (SPR). This method requires the use of materials such as gold, which is expensive thereby adding to the total cost of the fibre. Moreover, some SPR-based THz PCFs require the use of adhesives which may increase fabrication difficulties. The proposed fibre consists of a simple cladding and a single liquid channel in the core. Also, the proposed fibre neither requires the use of rare earth materials nor adhesives. The large elliptical core can be selectively infiltrated with liquid cocaine analyte by using direct manual glueing under a microscope. This is done by pressurising ultraviolet curable polymer inside the cladding air holes. To ensure the liquid enters only the core and not the cladding, the liquid may be slowly fed into the fibre from a fine tip such as a hypodermic needle. More recently, Luo *et al.* [28] and Gerosa *et al.* [29] have experimentally shown that the fabrication of PCF structures with liquid-filled cladding/core holes can be efficiently accomplished by using similar methods.

The performance of the proposed fibre may be characterised by the obtained relative sensitivity and detection limit [27]. The detection limit depends on the resolution of the measuring equipment but also on the sharpness of the interrogated spectral feature, for instance, the full-width at half-maximum of a Lorentzian-type resonance. Furthermore, the proposed fibre benefits greatly from already established techniques in standard optical fibre sensors based on the shifting of resonances stemming from fibre Bragg (FBG) or long-period gratings (LPGs), which rely on the phase matching and coupling between the fundamental guided mode and counter-propagating or cladding modes, respectively. Due to advances in optical fibre and material engineering, the proposed fibre can be integrated with FBG using a variety of techniques, such as direct laser writing, electric arc discharge, or by mechanical pressure for LPG.

An advantage of this method over other PCF fabrication methods is that, by moulding the preforms, large scale creation of a wide range of PCF geometries including an elliptical shape in various dimensions, is possible. Furthermore, since preform casting

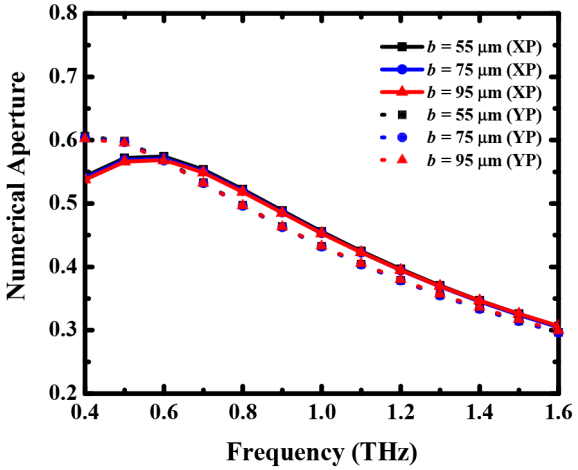

Fig. 8 *Numerical aperture with respect to frequency, for x and y polarisation modes at different minor axis length values*

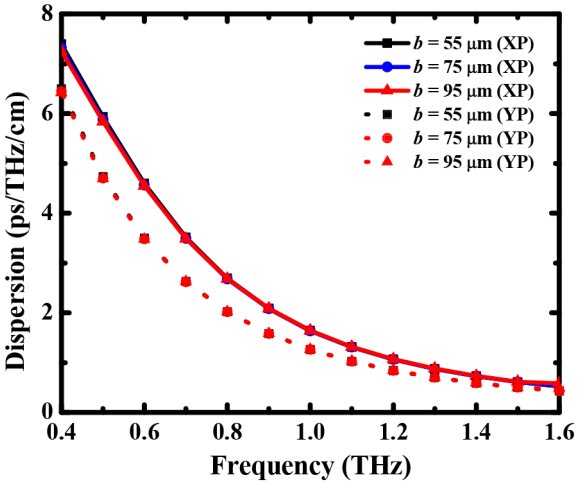

Fig. 9 *Dispersion profile of proposed PCF at different minor axis length value*

Table 1 Comparison with prior sensors

Ref.	Liquid sample	*r*, %	EML cm^{-1}	Freq. /Wave
[17]	ethanol	53.22	—	1.33 μm
[18]	plasma	77.96	—	1.30 μm
[19]	ethanol	85.7	—	1.6 THz
[20]	ethanol	68.87	0.05	1.0 THz
[21]	cyanide	77.5	0.023	1.8 THz
proposed PCF sensor	cocaine	87.02	0.009	1.0 THz

is done in sealed vessels, the method protects PCFs from probable physical and chemical contamination, which may increase scattering losses caused by optical inhomogeneity [30].

6 Conclusion

The Zeonex-based asymmetric PCF with a large single elliptical core and hexagon-shaped cladding is proposed for sensing liquid cocaine using terahertz waves. The full vector FEM with anisotropic PML boundary condition is employed for numerical analysis. With optimum design parameters found at 1 THz and $b = 95$ μm minor axis length, the proposed PCF exhibits low confinement loss of 1.95×10^{-3} cm^{-1} and 9.42×10^{-4} cm^{-1}, high relative sensitivity of 87.02 and 85.82% and extremely low EML of 0.009 and 0.012 cm^{-1} for the *x* and *y* polarisation modes, respectively. Furthermore, the fibre demonstrates high birefringence, large effective mode area and high numerical aperture. The introduction of the large core ellipse not only induces birefringence but also helps in accommodating a large amount of cocaine for sensing purposes. The proposed fibre may be fabricated in large quantities using the preform casting method. Thus, it is envisaged that the proposed sensor will broaden research possibilities in terahertz wave propagation and sensing liquid cocaine.

7 References

[1] Mehrvar, M., Bis, C., Scharer, J.M., *et al.*: 'Fiber-optic biosensors – trends and advances', *Anal. Sci.*, 2000, **16**, pp. 677–692

[2] Chen, T., Schultz, Z.D., Levin, I.W.: 'Infrared spectroscopic imaging of latent fingerprints and associated forensic evidence', *Analyst*, 2009, **134**, (9), pp. 1902–1904

[3] Smolik, G.M., Hvozdara, L., Di Francesco, J., *et al.*: 'Cocaine detection in liquid using a fibered platform and a mid-infrared quantum cascade laser', *Opt. Sens.*, 2014, **2014**, pp. 3–5

[4] Russell, P.: 'Photonic crystal fibers', *Science*, 2003, **299**, (5605), pp. 358–362

[5] Yakasai, I.K., Rahman, A., Abas, P.E., *et al.*: 'Theoretical assessment of a porous core photonic crystal fiber for terahertz wave propagation', *J. Opt. Commun.*, 2018, pp. 1–11

[6] Yakasai, I.K., Abas, P.E., Ali, S., *et al.*: 'Modelling and simulation of a porous core photonic crystal fibre for terahertz wave propagation', *Opt. Quantum Electron.*, 2019, **51**, (4), pp. 1–16

[7] Algorri, J.F., Zografopoulos, D.C., Tapetado, A., *et al.*: 'Infiltrated photonic crystal fibers for sensing applications', *Sensors*, 2018, **18**, pp. 1–32

[8] Begum, F., Abas, P.E.: 'Near infrared supercontinuum generation in silica based photonic crystal fiber', *Prog. Electromagn. Res. C*, 2019, **89**, pp. 149–159

[9] Islam, M.S., Sultana, J., Dinovitser, A., *et al.*: 'A novel Zeonex based oligoporous-core photonic crystal fiber for polarization preserving terahertz applications', *Opt. Commun.*, 2018, **413**, pp. 242–248

[10] Begum, F., Namihir, Y.: 'Photonic crystal fiber for medical applications', Yasin, M. (Ed.): '*Recent progress in optical fiber research*', (Intech, Croatia, 2012), pp. 229–246

[11] Pan, R., Zhao, S., Shen, J.: 'Terahertz spectra applications in identification of illicit drugs using support vector machines'. Proc. Eng., Nakhonphanom, Thailand, 2010, pp. 15–21

[12] Yakasai, I., Abas, P.E., Kaijage, S.F., *et al.*: 'Proposal for a quad-elliptical photonic crystal fiber for terahertz wave guidance and sensing chemical warfare liquids', *Photonics.*, 2019, **6**, (3), pp. 1–16

[13] Begum, F., Namihira, Y., Razzak, S.M.A., *et al.*: 'Novel broadband dispersion compensating photonic crystal fibers: applications in high-speed transmission systems', *Opt. Laser Technol.*, 2009, **41**, (6), pp. 679–686

[14] Wu, D.K.C., Kuhlmey, B.T., Eggleton, B.J.: 'Ultra-sensitive photonic crystal fiber refractive index sensor', *Opt. Lett.*, 2009, **34**, (3), pp. 322–324

[15] Park, J., Lee, S., Kim, S., *et al.*: 'Enhancement of chemical sensing capability in a photonic crystal fiber with a hollow high index ring defect at the center', *Opt. Express*, 2011, **19**, (3), pp. 1921–1929

[16] Ahmed, K., Asaduzzaman, S., Arif, F.H.: 'Numerical analysis of O-PCF structure for sensing applications with high relative sensitivity'. 2015 2nd Int. Conf. on Electrical Information and Communication Technologies (EICT), Khulna, Bangladesh, 2015, pp. 254–258

[17] Islam, M.S., Paul, B.K., Ahmed, K., *et al.*: 'Liquid-infiltrated photonic crystal fiber for sensing purpose: design and analysis', *Alexandria Eng. J.*, 2018, **57**, (3), pp. 1459–1466

[18] Islam, M.T., Moctader, M.G., Ahmed, K., *et al.*: 'Benzene shape photonic crystal fiber based plasma sensor: design and analysis', *Photonic Sens.*, 2018, **8**, (3), pp. 263–269

[19] Islam, M.S., Sultana, J., Ahmed, K., *et al.*: 'A novel approach for spectroscopic chemical identification using photonic crystal fiber in the terahertz regime', *IEEE Sens. J.*, 2018, **18**, (2), pp. 575–582

[20] Sultana, J., Islam, M.S., Ahmed, K., *et al.*: 'Terahertz detection of alcohol using a photonic crystal fiber sensor', *Appl. Opt.*, 2018, **57**, (10), p. 2426

[21] Islam, M.S., Sultana, J., Dinovitser, A., *et al.*: 'Sensing of toxic chemicals using polarized photonic crystal fiber in the terahertz regime', *Opt. Commun.*, 2018, **426**, pp. 341–347

[22] Davies, A.G., Burnett, A.D., Fan, W., *et al.*: 'Terahertz spectroscopy of explosives and drugs', *Mater. Today*, 2008, **11**, pp. 18–26

[23] Burnett, A.D., Fan, W., Upadhya, P.C., *et al.*: 'Broadband terahertz time-domain spectroscopy of drugs-of-abuse and the use of principal component analysis', *Analyst*, 2009, **134**, (8), pp. 1658–1668

[24] Kabir Yakasai, I., Abas, P.E., Begum, F.: 'Proposal of novel photonic crystal fibre for sensing adulterated petrol and diesel with kerosene in terahertz frequencies', *IET Optoelectron.*, 2020, **206**, pp. 1–9

[25] Yakasai, I.K., Abas, P.E., Suhaimi, H., *et al.*: 'Low loss and highly birefringent photonic crystal fibre for terahertz applications', *Optik*, 2020, **206**, p. 164321

[26] Paul, B., Haque, M., Ahmed, K., *et al.*: 'A novel hexahedron photonic crystal fiber in terahertz propagation: design and analysis', *Photonics.*, 2019, **6**, (1), p. 32

[27] Kuhlmey, B.T., Eggleton, B.J., Wu, D.K.C.: 'Fluid-filled solid-core photonic bandgap fibers', *J. Lightwave Technol.*, 2009, **27**, pp. 1617–1630

[28] Luo, M., Liu, Y., Wang, Z., *et al.*: 'Twin-resonance-coupling and high sensitivity sensing characteristics of a selectively fluid-filled microstructured optical fiber', *Opt. Express*, 2013, **21**, (25), p. 30911

[29] Gerosa, R.M., Spadoti, D.H., de Matos, C.J.S., *et al.*: 'Efficient and short-range light coupling to index-matched liquid-filled hole in a solid-core photonic crystal fiber', *Opt. Express*, 2011, **19**, (24), p. 24687

[30] Islam, M.S., Cordeiro, C.M.B., Franco, M.A.R., *et al.*: 'Terahertz optical fibers [invited]', *Opt. Express*, 2020, **28**, (11), p. 16089